Electromagnetic Modeling of Electronic Device by Electrical Circuit Parameters

Diego De Moura and Adroaldo Raizer

Department of Electrical Engineering
Federal University of Santa Catarina, Florianópolis, 88040-970, Brazil
diegodemouraa@gmail.com, adroaldo.raizer@ufsc.br

Abstract ─ This article proposes an electric model to determine the values of the electric fields of an electronic device. When applying the method, the integrated circuit device will be modeled on the resistance, inductance and capacitance values (R, L, C parameters) provided by the IBIS (*Input/Output Buffer Information Specification*), also considering the internal activity of the integrated circuit. The electric parameters of the printed circuit board tracks will be extracted by software based on the moments method and fast multipole method. Simulations of the electric model are performed in the time and frequency domain by the Fourier transform, and from the obtained harmonics, the values of the electric fields are calculated with software based on the finite elements method. Measurements were performed in order to validate the simulations.

Index Terms─Electrical circuit parameters, electromagnetic modeling, electronic device, IBIS model, internal activity.

I. INTRODUCTION

Problems related to electromagnetic compatibility (EMC) have increased significantly in recent decades, due to the increase of commutation speed and level of integration of electronic devices.

From this perspective, studies concerning the electromagnetic compatibility of electronic devices through numerical modeling have intensified.

The first significant contribution towards noise modeling of electronic components was with the IBIS model in the 90s, which proposed a standardized description of the electric performance of the input/output structures in integrated circuits [1].

Since then, the IBIS model has been improved and used in research aiming to diminish the problems with noise in electronic devices [2], [3], [4].

Despite the constant improvement of the IBIS models, the information provided for the internal activity of integrated circuits has limitations regarding their application in the EMC area.

This way, other models based on circuit parameters have been proposed to predict the electromagnetic emission of electronic components. In Japan, the IMIC model *(Interface Model for Integrated Circuits)* was proposed with the aim of standardizing the terminals and operation signals of integrated circuits [5]. Japanese researchers also propose the LECCS model (*Linear Equivalent Circuit and Current Source*), in which circuit parameters are used in order to model the core of integrated circuits, also considering the internal activity model by sources of current [6], [7].

At the same time in France, the standardization of components is proposed through the ICEM model (*Integrated Circuit Emission Model*). Being that the structure of this model also uses sources of current to model the internal activity (IA) of the integrated circuit, and in addition, PDN (*The Passive Distribution Network*) models are used to model the power source and decoupling capacitors of the IC's [8].

Based on the proposal of the LECCS and ICEM models, a range of studies are proposed in the setting of electromagnetic modeling of integrated circuits. Thus, in [9], [10], [11] the LECCS model is used to analyze conducted emission of microcontrollers, power sources and FPGA, respectively.

From the same conception in [12], the ICEM model is used to analyze the emission of microcontroller circuits. Whereas in [13], the characterization and modeling of CMOS circuit emissions is performed. Also, in [14], a model for determining conducted emission of the integrated circuit is proposed up to the frequency of 3 GHz. Being that comparisons are made with the ICEM model.

Although the LECCS, ICEM and other cited models, provide the constant advance of the EMC area applied to integrated circuits, their application are usually related to chip-level modeling.

Also in [15], [16], [17], [18], studies on electromagnetic modeling are performed through the partial element equivalent circuit (PEEC method). Through this method, the problem is transferred from the electromagnetic domain to the circuit domain, where conventional circuit simulator can be utilized to analyze the equivalent circuit. Usually the extracted circuit is not used to determine the

Submitted On: June 1, 2015
Accepted On: November 8, 2015

electric fields.

In this work, the modeling by electrical circuit parameters is used to determine the electromagnetic emission of the printed circuit board of the electronic device, with the integrated circuit device being modeled after the R, L, C parameters provided by the IBIS model. In addition, in order to model the internal activity of the IC, a voltage source is used. The R, L, C models of the tracks will be extracted by software based on the moments method and fast multipole method.

The signal circuit simulations are performed from the patterned electrical circuit in the time and frequency domain by Fourier transformation. Through the harmonics obtained, the electric fields (E) along the distance variation are calculated by software based on the finite elements method.

Aiming to validate the simulations, measurements of the signals are also performed in the time and frequency domain by the digital oscilloscope. The electric fields (E) are measured at distances close to the electronic device through a near-field probe. Whereas, in order to obtain the far-field values, measurements will be made in a gigahertz transverse electromagnetic (GTEM) cell.

II. ELECTRONIC DEVICE SELECTION

To demonstrate the effectiveness of the proposed methodology, an electronic device with emission source characteristics is selected. Such device, seen in Fig. 1 and Fig. 2, consists of a printed circuit board 13 cm long by 3 cm wide, of FR4 dielectric material with $\varepsilon = 4.4$ (relative electric permittivity). The circuit tracks are of microstrip topology made of copper (conductivity 58.10^6 S/m).

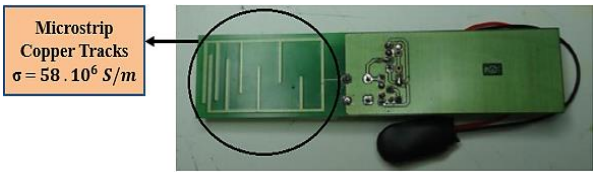

Fig. 1. Bottom view of the electronic device.

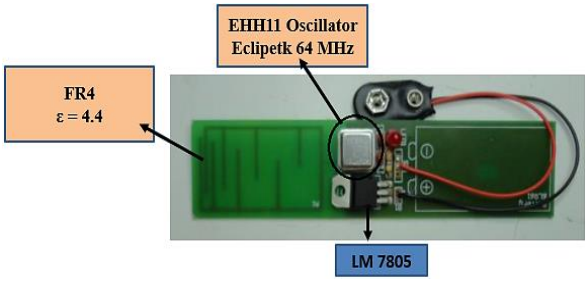

Fig. 2. Top view of the electronic device

Besides that, the circuit consists of a trapezoidal signal oscillator (EHH11-Eclipetk) responsible for generating the excitation signal of the tracks in the 64 MHz frequency [19]. The supply of the circuit (5V) is performed by a 9V battery connected to the circuit through an LM7805 voltage regulator.

The choice of device was motivated by the fact that printed circuit board tracks excited by trapezoidal signals are responsible for generating a multiplicity of harmonic components. These components are usually mechanisms which cause EMC problems [20].

III. MODELING AND NUMERICAL SIMULATIONS OF ELECTRONIC DEVICE

The modeling of EHH11 oscillator circuit was performed using the IBIS model supplied by the manufacturer (Eclipetk) [21]. Among the features that this model provides are the die (semiconductor) capacitance values information referenced as (Ccomp), and also the R, L, C parameters of the integrated circuit pins.

The IBIS model of clock pin for the EHH11 oscillator signal in circuit format can be seen in Fig. 3. The values provided by the model for the pin are: inductance (LCLKOUT = 2.90 *nH*), capacitance (CCLKOUT = 0.85 *pF*) and resistance (RCLKOUT = 75 *m* Ω). It is also possible to view the value provided for the capacitance of the (die) semiconductor (Ccomp_CLKOUT = 1.70 *pF*).

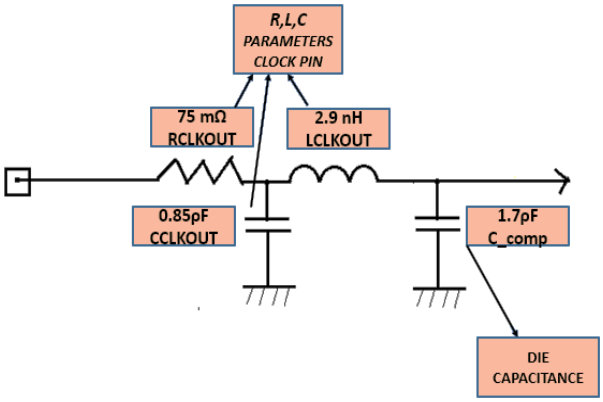

Fig. 3. Clock pin representation by the IBIS model.

The extraction of the R, L, C parameters of the device tracks was performed using the software based on the boundary element method (moments method) and fast multipole method [22]. Multipole acceleration can reduce required computation time extracting parameters R, L, C of printed circuit boards [30], [31], [32].

As it is possible to see in Fig. 4, the values obtained for the frequency of 64 *MHz* are, L = 62.336 *nH*, C = 1.9917 *pF* and R = 0.18235 Ω. For the circuit representation the equivalent π model was used, in which $C_1 = C_2 = \frac{C}{2}$.

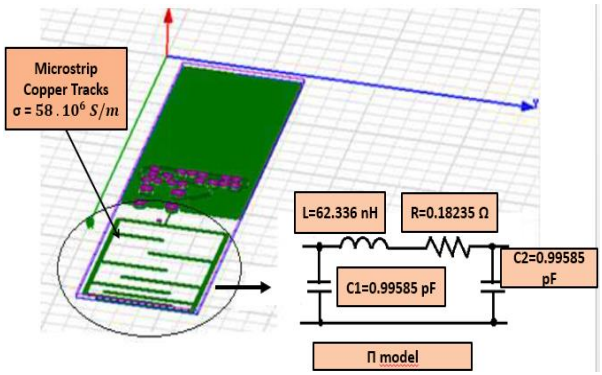

Fig. 4. R, L, C tracks circuit.

It is possible to observe that firstly the modeling of the output pin of the signal through the R, L, C parameters provided by the IBIS model of the EHH11 component was performed. Subsequently, the R, L, C parameters of the tracks were extracted. And in order for the circuit to be capable of simulation, the IBIS model of the IC was connected to the model of the tracks. In addition, a voltage source (clock) was connected in the internal capacitance of the semiconductor (die) of the integrated circuit (Ccomp_CLK) = 1.70 *pF*) which represents the model of the internal activity of the IC. Also, through simulations, the circuit load was determined *RL* = 100 Ω. The electric circuit in its final modeling can be seen in Fig. 5 [23].

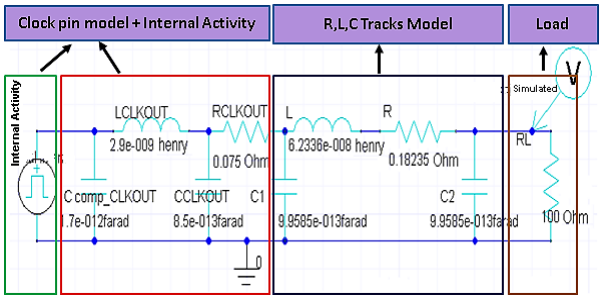

Fig. 5. Model of the electronic device by circuit parameters.

The signal circuit simulations are performed from the patterned electrical circuit in the time and frequency domain by Fourier transformation. As seen in Fig. 6, the signal obtained in the time domain in the 100 Ω load has the following specifications: amplitude $V = 5\ V$, rise time t_r = 2.391 *ns*, fall time t_f = 1.762 *ns*, pulse width *PW* = 3.6595 *ns* and period *PER* = 15.625 *ns*.

The simulation performed in the frequency domain can be seen in Fig. 7. The analysis was directed toward a few odd harmonics 1st (64 MHz), 3rd (192 MHz), 5th (320 MHz), 7th (448 MHz), 9th (576 MHz) and 11th (704 MHz), usually resulting from trapezoidal signals.

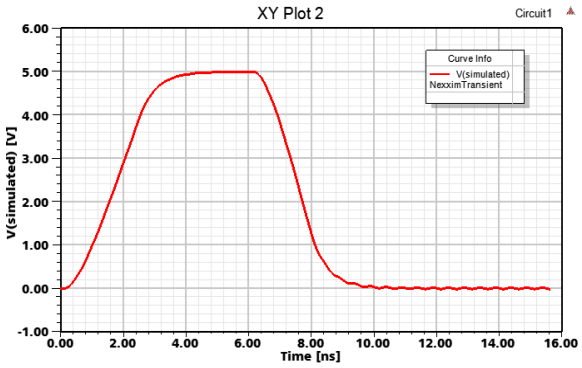

Fig. 6. Simulated signal in the time domain.

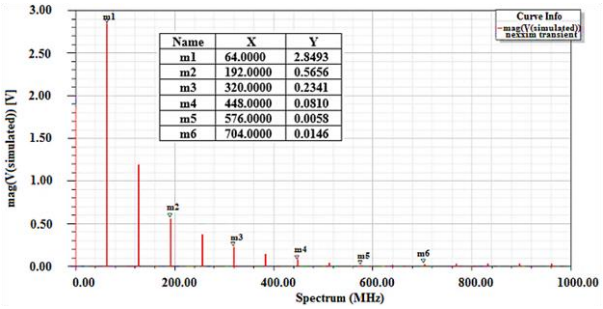

Fig. 7. Simulation in the frequency domain.

The calculations of electric fields as from the amplitudes of harmonics resulting from Fourier analysis were performed using the software based on the finite elements method (FEM) [24]. FEM is based on the differential formulation of Maxwell's equations [25], [26]. For the differential based techniques, the discretization of the complete computational domain is performed, this technique delivers predominantly the solution in field variables, i.e., $\vec{E}$ and $\vec{H}$. This is suitable for far and near field analysis [29].

As it can be seen in Fig. 8, the physical characteristics of the electronic device were modeled, such as dielectric constant of FR4 (ε = 4.4) and conductivity of the copper tracks (σ = 58.10^6 S/m). The boundary condition was also inserted around the device, i.e., an air box with permittivity and relative permeability equal to 1.0006 and 1, respectively.

Moreover, for solution dominion is used finite element boundary integral (FEBI) [28]. This condition allows the absorption of the incident field and not dependent on the incident angle.

The calculations of electric fields along the distance variations were performed using a test plan inserted in 8 different distances (1 cm, 2 cm, 4 cm, 10 cm, 20 cm, 30 cm and 300 cm) of the electronic device. Thus, the harmonics (1st, 3rd, 5th, 7th, 9th, and 11th) and their respective amplitudes were selected as excitation of the device tracks.

The simulations were performed in the basic frequency (64 MHz), third harmonic (192 MHz), fifth harmonic (320 MHz), seventh harmonic (448 MHz), ninth harmonic (576 MHz) and the eleventh harmonic (704 MHz).

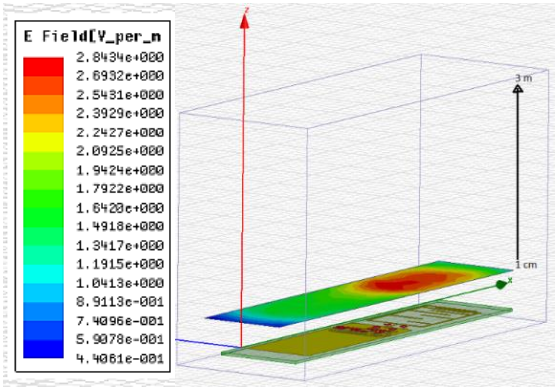

Fig. 8. Modeling and simulation of the electric fields.

IV. MEASUREMENTS OF THE ELECTRONIC DEVICE

In order to validate the results obtained from the simulations, signals measurements were performed in the time and frequency domain using a digital oscilloscope.

Figure 9 illustrates the specifics of the signal in the time domain: amplitude of 5,08 *V*, frequency equal to 64,06 *MHz*, period of 15,62 *ns*, rise and fall time equal to 2.214 *ns* and 1.707 *ns* respectively.

Upon confirming the operation of the signal in the time domain, analyses of the signal were performed in the frequency domain by the Fourier transform. In Fig. 10, the measurements of some harmonics resulting from the application of the transform are shown: 1ª (64 *MHz*), 3ª (192 *MHz*), 5ª (320 *MHz*), 7ª (448 *MHz*), 9ª (576 *MHz*) and 11ª (704 *MHz*). Their respective frequency values in (MHz) and amplitude in (V) are shown in Table 1.

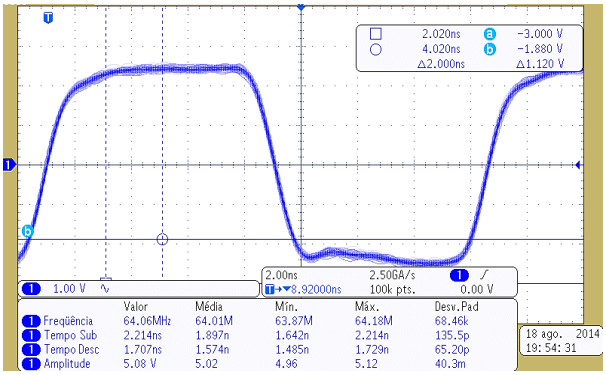

Fig. 9. Excitement signal in the time domain.

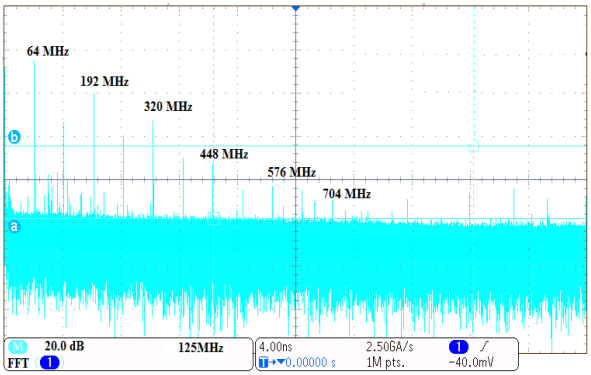

Fig. 10. Analysis of the signal in the frequency domain.

Measurements of the values of the electric fields (E_z) were also performed. For the near field region a near-field probe (HZ-14) was used, together with a field receptor (ESPC), allowing measurements of the electric field (E_z) values in the 9 kHz to 1 GHz range. It is worth noting that the probe has an antenna factor equal to 67 dBuV/m and is manufactured with an integrated amplifier which enables increase of gain [33].

In the configuration of the near field measurements illustrated in Fig. 11, it is possible to see the probe and fields receiver, both in a fixed position and the device under test moving at distances of 1 cm, 2 cm, 4 cm, 6 cm, 10 cm, 20 cm and 30 cm from the probe. Furthermore, in order to prevent electromagnetic fields from the outside environment to interfere with the measurements, a Faraday cage was used.

In the near field measurements are obtained through voltage induced values in the probe terminal and these values are added to the antenna factor, according to Equation (1):

$$|E|\,[dB\,(\mu\,V/m) = dB\,(\mu V) + AF\,]. \qquad (1)$$

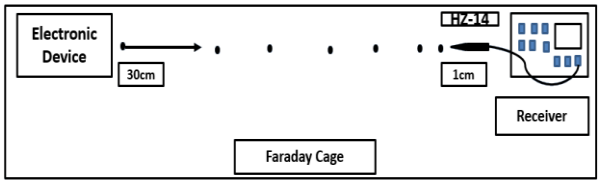

Fig. 11. Measurement setup for distances of 1 cm to 30 cm.

For measurements in the far-field region, a receiver and a GTEM cell were used. With the electronic device (EUT) properly positioned in the cell, close to the absorbers so as to center it between the conductive plate (septum) and the ground of the chamber, which are 100 cm apart. Thus, it is seen that d = 50 cm, as shown in Fig. 12.

Once the circuit is properly positioned, the peak value measurements of the of the electric far-fields (E_z) are performed in accordance with the (CISPR 22) standard, which is, Class B equipment, radiation range

of 30 MHz to 1 GHz and 3 m (300 cm) distance. Using the relationship ($\lambda/2\pi$), it is possible to conclude that for the frequency of 64 MHz, the distance of 3 m is considered far field region [34].

Measurements for the values of the near and far electric fields were performed for the previously analyzed harmonics. Fundamental frequency (64 MHz), third harmonic (192 MHz), fifth harmonic (320 MHz), seventh harmonic (448 MHz), ninth harmonic (576 MHz) and the eleventh harmonic (704 MHz).

The measurement results for the values of the electric field (E_z) in dBμV/m due to the distance variation in (cm) for each of the aforesaid frequencies, are compared to the simulations and shown below.

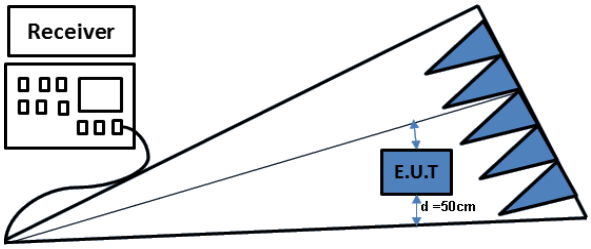

Fig. 12. Measurement GTEM for 3-meter distance.

V. COMPARISONS BETWEEN SIMULATED AND MEASURED RESULTS

The results obtained through numerical simulations were compared with the measurements made in the laboratory.

Firstly, the device excitation signals (64 MHz) in the time domain were compared, as shown in Fig. 13. It is possible to observe through the purple signal (measured signal) that it has the following characteristics: period (15,62 *ns*), amplitude 5 *V*, rise and fall time equal to 2.2 *ns* and 1.7 *ns* respectively. By making the comparison of the measured signal with the simulated signal (red signal), it is concluded that it has the same characteristics as the measured signal.

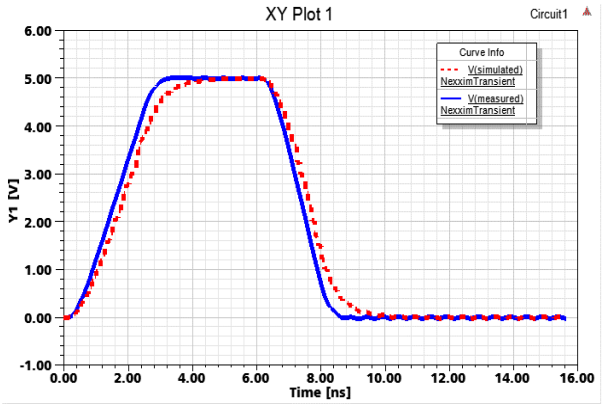

Fig. 13. Comparison of the signals in the time domain.

Afterwards, the amplitudes of the harmonics in the frequency domain were compared. As analysis of Table 1 shows, it is possible to observe that the 1st harmonic presents a difference in amplitude of (0.3493 *V*), the 3rd (0.0756 *V*), the 5th (0.0741 *V*), the 7th (0.063 *V*) the 9th (0.0092 *V*) and the 11th (0.0046 *V*).

Table 1: Comparison of the signal amplitudes in the frequency domain

Frequency (MHz)	Amplitude of the Measured Signal (V)	Amplitude of the Simulated Signal (V)	Differences of Amplitude |V|
64 (1st)	2.5	2.8493	|0.3493|
192 (3rd)	0.49	0.5656	|0.0756|
320 (5th)	0.16	0.2341	|0.0741|
448 (7th)	0.018	0.0810	|0.063|
576 (9th)	0.015	0.0058	|0.0092|
704 (11th)	0.01	0.0146	|0.0046|

Finally, the values of the measured and simulated electric fields were confronted, as shown in Figs. 14, 15, 16, 17, 18 and 19. The values of electric field were used in measurements and simulations, because these variables are usually used in the normative references of electromagnetic emission of electronic devices [27].

It is noted by the measured values (blue curve) and simulated values (red curve), that the values of the electric fields (E_z) in (dBμV/m) over the distance variation, in (cm), show great similarity. However, the most significant differences are observed in the 7th harmonic (448 MHz) or 20 cm (10.96 *dBμV/m*), 30 cm (10.73 *dBμV/m*) as shown in Fig. 16 and 9th harmonic (576 MHz), or 1 cm (9.88 *dBμV/m*) 2 cm (10.7 *dBμV/m*), 4 cm (9.72 *dBμV/m*), 6 cm (9.59 *dBμV/m*), 10 cm (9.1 *dBμV/m*) and 20 cm (6.52 *dBμV/m*) as shown in Fig. 17.

In other words, analyzing the difference between the amplitudes of the seventh and ninth harmonic in dB, were obtained |13.1| dB for seventh harmonic and |8.2| dB for the ninth harmonic, as shown in Table 2. Therefore, the most significant differences in the values of electric fields were observed for the same.

In addition, the near-field probe model of the GTEM cell and measurement uncertainties were not considered. Thus, such factors may also have caused the discrepancies between the amplitude values of the electric fields (E).

Table 2: Comparing the amplitudes of the seventh and ninth harmonic in dB

Frequency (MHz)	Amplitude of the Measured Signal V→dB	Amplitude of the Simulated Signal V→dB	Differences of Amplitude |dB|
448 (7th)	(0.018 V) = -34.9 dB	(0.0810) = -21.8 dB	|13.1|
576 (9th)	(0.015) = -36.5 dB	(0.0058) = -44 dB	|8.2|

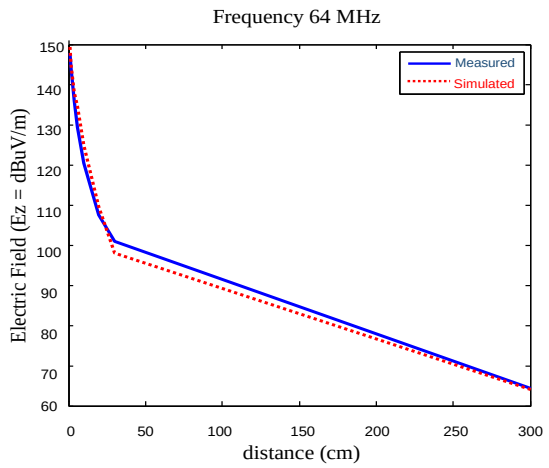

Fig. 14. Comparisons between electric fields measured and simulated for the 64 MHz frequency.

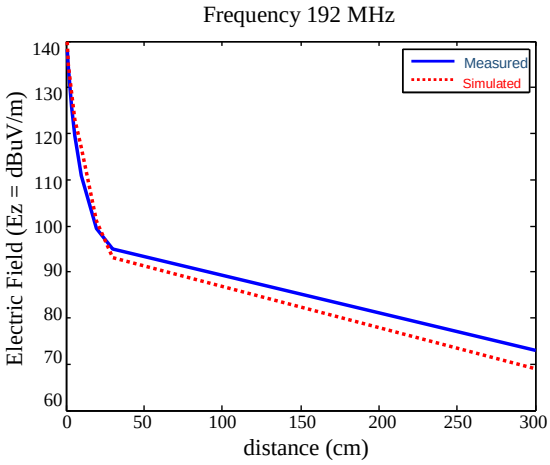

Fig. 15. Comparisons between electric fields measured and simulated for the 192 MHz frequency.

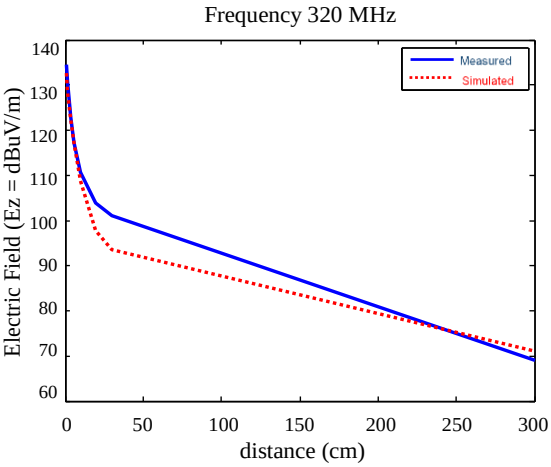

Fig. 16. Comparison between electric fields measured and simulated for the 320 MHz frequency.

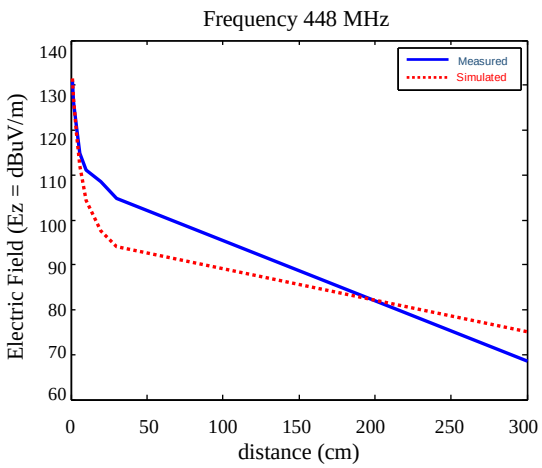

Fig. 17. Comparison between electric fields measured and simulated for the 448 MHz frequency.

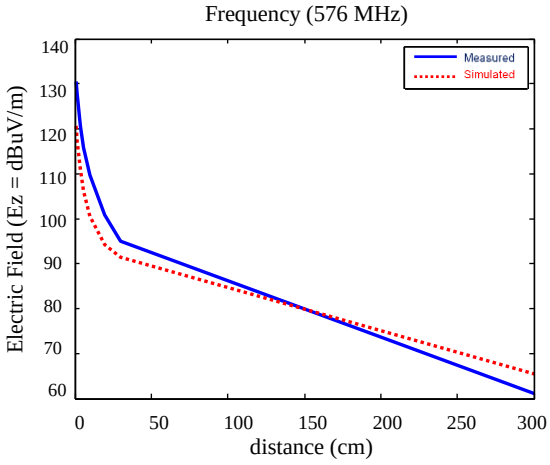

Fig. 18. Comparison between electric fields measured and simulated for the 576 MHz frequency.

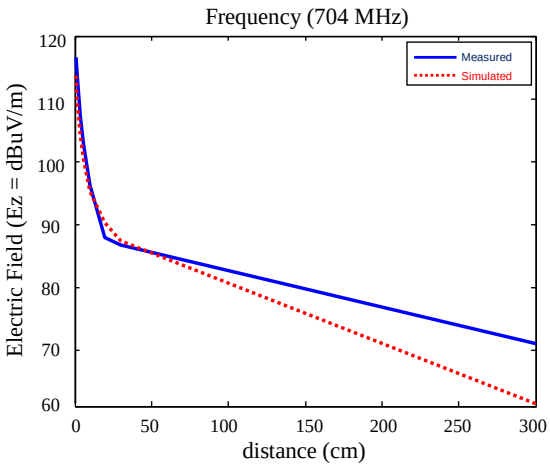

Fig. 19. Comparison between electric fields measured and simulated for the 704 MHz frequency.

VI. CONCLUSION

This article has demonstrated a new methodology for the analysis of electric fields by an electronic device. The technique applied incorporates a complete modeling of the electronic device, in which the integrated circuit is modeled after the IBIS model, also considering its internal activity model. In addition, the R, L, C parameters of the tracks are extracted.

Thus, this way it is possible to obtain an electric and simulated circuit, enabling the determination of the signals in the time and frequency domain, and consequently, the values of electric fields can be determined by simulation based on the finite elements method.

From the obtained results, it can be said that the proposed methodology, can be a starting point for standardized models of printed circuit boards in determining the electromagnetic emission of the same.

REFERENCES

[1] IBIS, Electronic Behavioral Specifications of Digital Integrated Circuits I/O Buffer Information Specification, International Electrotechnical Commission (IEC) 62014-1, 2003.

[2] P. Pulici, A. Girardi, G. P. Vanalli, R. Izzi, G. Bernardi, G. Ripamonti, A. G. M. Strollo, and G. Campardo, "A modified IBIS model aimed at signal integrity analysis of systems in package," *IEEE Transactions on Circuits and Syst*., vol. 55, no. 7, pp. 1921-1928, Aug. 2008.

[3] B. B. M'Hamed, F. Torrès, A. Reineix, and P. Hoffmann, "Complete time-domain diode modeling: application to off-chip and on-chip protection devices," *IEEE Trans. on Electromagn. Compat.*, vol. 53, no. 2, pp. 349-365, May 2011.

[4] N. Monnereau, F. Caignet, N. Nolhier, M. Bafleur, and D. Tremouilles, "Investigation of modeling system ESD failure and probability using IBIS ESD models," *IEEE Trans. on Device and Materials Reliability*, vol. 12, no. 4, pp. 599-606, Dec. 2012.

[5] I/O Interface Model for Integrated Circuits (IMIC), International Electrotechnical Commission (IEC) 62404, 2003.

[6] O. Wada, Y. Fukumoto, H. Osaka, W. Zhi Liang, O. Shibata, S. Matsunaga, T. Watanabe, E. Takahashi, and R. Koga, "High-speed simulation of PCB emission and immunity with frequency-domain IC/LSI source models," in Proc. *IEEE Int. Symp. Electromagn. Compat.*, vol. 1, pp. 4-9, 2003.

[7] K. Ichikawa, M. Inagaki, Y. Sakurai, I. Iwase, M. Nagata, and O. Wada, "Simulation of integrated circuit immunity with LECCS model," in Proc. *17th Int. Symp. Electromagn. Compat*., Zurich, Switzerland, pp. 308-311, 2006.

[8] Integrated Circuits Emission Model (ICEM), International Electrotechnical Commission (IEC) 62014-3, 2004.

[9] K. Iokibe, R. Higashi, T. Tsuda, K. Ichikawa, K. Nakamura, Y. Toyota, and R. Koga, "Modeling of microcontroller with multiple power supply pins for conducted EMI simulations," in Proc. *2012 IEEE Int. Symp. Electrical Design of Advanced Packaging and Systems*, Seoul, Korea, pp. 135-138, 2008.

[10] T. Ibuchi and T. Funaki, "A study on EMI noise source modeling with current source for power conversion circuit," in Proc. *2012 IEEE Int. Symp. Electromagn. Compat*., EMCEUROPE, Rome, Italy, pp. 1-6, 2012.

[11] K. Iokibe and Y. Toyota, "Estimation of data-dependent power voltage variations of FPGA by equivalent circuit modeling from on-board measurements," in Proc. *2013 Int. Workshop Electromagn. Compat. Integr. Circuits*, EMCCOMPO, Nara, Japan, pp. 175-179, 2013.

[12] C. Labussière-Dorgan, S. Bendhia, E. Sicard, J. Tao, H. J. Quaresma, C. Lochot, and B. Vrignon, "Modeling the electromagnetic emission of a microcontroller using a single model," *IEEE Trans. on Electromagn. Compat*., vol. 50, no. 1, pp. 22-34, Feb. 2008.

[13] B. Vrignon, S. Delmas Bendhia, E. Lamoureux, and E. Sicard, "Characterization and modeling of parasitic emission in deep submicron CMOS," *IEEE Trans. on Electromagn. Compat.*, vol. 47, no. 2, pp. 382-387, May 2005.

[14] N. Berbel, R. F. Garcia, and I. Gil, "Characterization and modeling of the conducted emission of integrated circuits up to 3 GHz," *IEEE Trans. on Electromagn. Compat.*, vol. 56, no. 4, pp. 382-387, Aug. 2014.

[15] D. Daroui and J. Ekman, "Parallel implementation of the PEEC method," *Journal of Applied Computat. Electromag. Society*, vol. 25, no. 5, pp. 410-422, 2010.

[16] G. Antonini, "Fast multipole formulation for PEEC frequency domain modeling," *Journal of Applied Computat. Electromag. Society*, vol. 17, no. 3, Nov. 2002.

[17] D. Daroui and J. Ekman, "Efficient PEEC-based simulations using reluctance method for power electronic applications," *Journal of Applied Computat. Electromag. Society*, vol. 27, no. 10, pp. 830-841, 2012.

[18] F. Freschi and M. Repetto, "A general framework for mixed structured/unstructured PEEC modelling," *Journal of Applied Computat. Electromag. Society*, vol. 23, no. 3, pp. 200-206, 2008.

[19] (2014). [Online]. Available: http://www.ecliptek.com/oscillators/EHH11/.

[20] H. W. Ott, *Noise Reduction Techniques in Electronic Systems*, 2nd ed., New York: Wiley-Interscience, 1988.
[21] (2014). [Online]. Available: http://www.ecliptek.com/IBIS/ehh11a.ibs.
[22] Ansys Q3D Extractor, ver. 15.0, Ansys Corporation, Canonsburg, PA, Estados Unidos, 2014.
[23] Ansys Designer, ver. 8.0, Ansys Corporation, Canonsburg, PA, Estados Unidos, 2012.
[24] Ansys High Frequency Structure Simulation (HFSS), ver. 15.0, Ansys Corporation, Canonsburg, PA, Estados Unidos, 2014.
[25] Z. J. Cendes, "Vector finite elements for electromagnetic field computation," *IEEE Trans. Magnetics*, vol. 27, pp. 3958-3966, Sep. 1991.
[26] Z. J. Cendes and J. F. Lee, "The transfinite element method for modeling MMIC devices," *IEEE Trans. on MTT*, vol. 36, pp. 1639-49, Dec. 1988.
[27] *Radio Disturbance and Immunity Measuring Apparatus*, CISPR 22, ed. 6, International Electrotechnical Commission (2008).
[28] J. Liu and J.-M. Jin, "A novel hybridization of higher order finite element and boundary integral methods for electromagnetic scattering and radiation problems," *IEEE Trans. Antennas Propagat*., vol. 49, no. 12, pp. 1794-1806, Dec. 2001.
[29] J. Ekman, *Electromagnetic Modeling Using the Partial Element Equivalent Circuit Method*, Ph.D. Theses, EISLAB, LuleÂ, Sweden, 2003.
[30] X. Wang, D. Liu, W. Yu, and Z. Wang, "Improved boundary element method for fast 3-D interconnect resistance extraction," *IEICE Trans. on Electronics*, vol. E88-C, no. 2, pp. 232-240, Feb. 2005.
[31] K. Nabors and J. White, "FastCap: a multipole accelerated 3-D capacitance extraction program," *IEEE Trans. Computer-Aided Design*, vol. 10, no. 11, pp. 1447-1459, 1991.
[32] M. Kamon, M. J. Tsuk, and J. K. White, "Fasthenry: a multipole accelerated 3-D inductance extraction program," *IEEE Trans. Microwave Theory Tech*., pp. 1750-1758, Sep. 1994.
[33] (2015) [Online] https://www.rohde-schwarz.com/en/product/hz-14_3-productstartpage_63493-11717.html.
[34] A. C. Balanis, Antenna Theory Analysis and Design, 3rd ed., New Jersey, John Wiley & Sons, Inc.

Diego de Moura was born in Chapecó, Santa Catarina, Brazil, in 1982. He received the degree in Electronic Systems from the Federal Institute of Santa Catarina, Brazil, in 2007, and Master's degree in Electrical Engineering from the Federal University of Santa Catarina, Brazil, in 2011. He is currently a doctoral student in Electrical Engineering of the Federal University of Santa Catarina. His current research interests are electromagnetic fields, electromagnetic compatibility, and electromagnetic modeling of electronic systems.

Adroaldo Raizer was born in Lages, Santa Catarina, Brazil, on August 11, 1963. He received the B.E. (1985) and M.E. (1987) degree in Electrical Engineering from Federal University of Santa Catarina, Brazil, and the Doctor's degree (1991) from Institut National Polytechnique de Grenoble, France. Raizer is currently a Full Professor of the Electrical Engineering Department at Federal University of Santa Catarina, Brazil. His current research interests are electromagnetic fields, electromagnetic compatibility, and numerical methods.